

New Measurement of $\frac{\text{BR}(D^+ \rightarrow \rho^0 \mu^+ \nu)}{\text{BR}(D^+ \rightarrow \bar{K}^{*0} \mu^+ \nu)}$ Branching Ratio

The FOCUS Collaboration ¹

J. M. Link ^a P. M. Yager ^a J. C. Anjos ^b I. Bediaga ^b
C. Castromonte ^b A. A. Machado ^b J. Magnin ^b A. Massafferri ^b
J. M. de Miranda ^b I. M. Pepe ^b E. Polycarpo ^b A. C. dos Reis ^b
S. Carrillo ^c E. Casimiro ^c E. Cuautle ^c A. Sánchez-Hernández ^c
C. Uribe ^c F. Vázquez ^c L. Agostino ^d L. Cinquini ^d
J. P. Cumalat ^d B. O'Reilly ^d I. Segoni ^d K. Stenson ^d
J. N. Butler ^e H. W. K. Cheung ^e G. Chiodini ^e I. Gaines ^e
P. H. Garbincius ^e L. A. Garren ^e E. Gottschalk ^e P. H. Kasper ^e
A. E. Kreymer ^e R. Kutschke ^e M. Wang ^e L. Benussi ^f
M. Bertani ^f S. Bianco ^f F. L. Fabbri ^f S. Pacetti ^f A. Zallo ^f
M. Reyes ^g C. Cawfield ^h D. Y. Kim ^h A. Rahimi ^h J. Wiss ^h
R. Gardner ⁱ A. Kryemadhi ⁱ Y. S. Chung ^j J. S. Kang ^j
B. R. Ko ^j J. W. Kwak ^j K. B. Lee ^j K. Cho ^k H. Park ^k
G. Alimonti ^l S. Barberis ^l M. Boschini ^l A. Cerutti ^l
P. D'Angelo ^l M. DiCorato ^l P. Dini ^l L. Edera ^l S. Erba ^l
P. Inzani ^l F. Leveraro ^l S. Malvezzi ^l D. Menasce ^l
M. Mezzadri ^l L. Moroni ^l D. Pedrini ^l C. Pontoglio ^l F. Prelz ^l
M. Rovere ^l S. Sala ^l T. F. Davenport III ^m V. Arena ⁿ G. Boca ⁿ
G. Bonomi ⁿ G. Gianini ⁿ G. Liguori ⁿ D. Lopes Pegna ⁿ
M. M. Merlo ⁿ D. Pantea ⁿ S. P. Ratti ⁿ C. Riccardi ⁿ P. Vitulo ⁿ
C. Göbel ^o J. Otalora ^o H. Hernandez ^p A. M. Lopez ^p
H. Mendez ^p A. Paris ^p J. Quinones ^p J. E. Ramirez ^p Y. Zhang ^p
J. R. Wilson ^q T. Handler ^r R. Mitchell ^r D. Engh ^s M. Hosack ^s
W. E. Johns ^s E. Luigi ^s J. E. Moore ^s M. Nehring ^s
P. D. Sheldon ^s E. W. Vaandering ^s M. Webster ^s M. Sheaff ^t

^aUniversity of California, Davis, CA 95616

^bCentro Brasileiro de Pesquisas Físicas, Rio de Janeiro, RJ, Brazil

- ^c*CINVESTAV, 07000 México City, DF, Mexico*
^d*University of Colorado, Boulder, CO 80309*
^e*Fermi National Accelerator Laboratory, Batavia, IL 60510*
^f*Laboratori Nazionali di Frascati dell'INFN, Frascati, Italy I-00044*
^g*University of Guanajuato, 37150 Leon, Guanajuato, Mexico*
^h*University of Illinois, Urbana-Champaign, IL 61801*
ⁱ*Indiana University, Bloomington, IN 47405*
^j*Korea University, Seoul, Korea 136-701*
^k*Kyungpook National University, Taegu, Korea 702-701*
^l*INFN and University of Milano, Milano, Italy*
^m*University of North Carolina, Asheville, NC 28804*
ⁿ*Dipartimento di Fisica Nucleare e Teorica and INFN, Pavia, Italy*
^o*Pontificia Universidade Católica, Rio de Janeiro, RJ, Brazil*
^p*University of Puerto Rico, Mayaguez, PR 00681*
^q*University of South Carolina, Columbia, SC 29208*
^r*University of Tennessee, Knoxville, TN 37996*
^s*Vanderbilt University, Nashville, TN 37235*
^t*University of Wisconsin, Madison, WI 53706*

Abstract

Using data collected by the FOCUS experiment at Fermilab, we present a new measurement of the charm semileptonic branching ratio $\frac{\text{BR}(D^+ \rightarrow \rho^0 \mu^+ \nu)}{\text{BR}(D^+ \rightarrow \bar{K}^{*0} \mu^+ \nu)}$. From a sample of 320 ± 44 and 11372 ± 161 $D^+ \rightarrow \rho^0 \mu^+ \nu$ and $D^+ \rightarrow \bar{K}^{*0} \mu^+ \nu$ events respectively, we find $\frac{\text{BR}(D^+ \rightarrow \rho^0 \mu^+ \nu)}{\text{BR}(D^+ \rightarrow \bar{K}^{*0} \mu^+ \nu)} = 0.041 \pm 0.006$ (stat) ± 0.004 (syst).

1 Introduction

Semileptonic decays provide an ideal environment for the study of hadronic matrix elements affecting the weak mixing angles from heavy flavor decays since the weak part of the current can be separated from the hadronic part of the current. The hadronic current, described by form factors, can be calculated by different theoretical methods, e.g., Lattice QCD (LQCD), Quark Model (QM), Sum Rules (SR), without the added complication of significant final state interactions. While many theoretical models predict the value for

¹ See <http://www-focus.fnal.gov/authors.html> for additional author information.

the branching ratio $\frac{\text{BR}(D^+ \rightarrow \rho^0 \ell^+ \nu)}{\text{BR}(D^+ \rightarrow \bar{K}^{*0} \ell^+ \nu)}$ [1,2,3,4,5,6,7,8,9,10,11,12], only a few experimental measurements of this ratio have been made. Furthermore, even though previous measurements of $\frac{\text{BR}(D^+ \rightarrow \rho^0 \mu^+ \nu)}{\text{BR}(D^+ \rightarrow \bar{K}^{*0} \mu^+ \nu)}$ have suffered from a lack of statistics [13,14,15], most theoretical predictions still differ by at least 2σ from the world average [16] for the muonic mode. In this paper, we present a new measurement of this branching ratio based on $320 \pm 44 D^+ \rightarrow \rho^0 \mu^+ \nu$ events.²

2 Event Selection

The data for this analysis were collected with the FOCUS experiment during the 1996–97 fixed target run at Fermilab. The FOCUS experiment utilized an upgraded version of the forward multi-particle spectrometer used by experiment E687 [17] to study charmed particles produced by the interaction of high energy photons, with an average energy of ~ 180 GeV, with a segmented BeO target. Precise vertex determination was made possible by two sets of silicon strips detectors consisting of two pairs of planes interleaved with the target segments [18] and four sets of planes downstream of the target region, each with three views. Five sets of proportional wire chambers combined with two oppositely polarized analysis magnets completed the tracking and momentum measurement system. Charged hadron identification was provided with three threshold multi-cell Čerenkov counters capable of separating kaons from pions up to 60 GeV/ c [19]. Muons were identified in the “inner” muon system, located at the end of the spectrometer, which consisted of six arrays of scintillation counters subtending approximately ± 45 mrad [20].

The $D^+ \rightarrow \rho^0 \mu^+ \nu$ events are selected by requiring two oppositely charged pions and a muon to form a good decay vertex with confidence level exceeding 5%. Tracks not used in the decay vertex are used to form candidate production vertices. Of these candidates, the vertex with the highest multiplicity is selected as the production vertex; ties are broken by selecting the most upstream vertex. This production vertex is required to have a confidence level greater than 1% and be inside the target material.

Muon tracks are required to have a minimum momentum of 10 GeV/ c and must have hits in at least five of the six planes comprising the inner muon system. These hits must be consistent with the muon track hypothesis with a confidence level exceeding 1%. In order to reduce contamination from in-flight decays of pions and kaons within the spectrometer, we require the muon tracks to have a confidence level greater than 1% under the hypothesis that the trajectory is consistent through the two analysis magnets.

The Čerenkov algorithm used for particle identification returns the negative

² Unless stated otherwise, charge conjugation is implied.

log-likelihood for a given track to be either an electron, pion, kaon, or proton. To identify the two pion candidates we require that no other hypothesis is favored over the pion hypothesis by more than five units of log-likelihood for each track. Furthermore, we require that the pion hypothesis for the track with charge opposite to the muon be favored over the kaon hypothesis by at least five units of log-likelihood. This very stringent is cut used to suppress background from the Cabibbo favored decay $D^+ \rightarrow K^- \pi^+ \mu^+ \nu$ where the kaon is misidentified as a pion. Additionally, the pion hypothesis must be favored over the kaon hypothesis by more than one unit of log-likelihood for the remaining track.

To suppress short-lived backgrounds, we require the decay vertex to be separated from the production vertex by at least 15 times the calculated uncertainty on the separation σ_L and be outside of the target material by 1σ . Because the target region has embedded detectors, the decay vertex is also required to be outside the detector material. These cuts are especially effective at removing non-charm backgrounds, making the contribution from minimum-bias events negligible. Contamination from higher multiplicity charm events is reduced by isolating the $\pi\pi\mu$ vertex from other tracks in the event (not including tracks in the primary). We require that the maximum confidence level for any other track to form a vertex with the candidate to be less than 1%.

Background from $D^{*+} \rightarrow D^0 \pi^+ \rightarrow (\pi^- \mu^+ \nu) \pi^+$, where the soft pion is erroneously assigned to the decay vertex, is reduced by requiring $M(\pi^+ \pi^- \mu^+) - M(\pi^- \mu^+) > 0.20 \text{ GeV}/c^2$. Background decay modes with a neutral hadron in the final state, such as $D_s^+ \rightarrow \eta' \mu^+ \nu \rightarrow (\eta \pi^+ \pi^+) \mu^+ \nu$, are reduced by requiring a visible mass cut of $1.2 \text{ GeV}/c^2 < M(\pi^+ \pi^- \mu^+) < 1.8 \text{ GeV}/c^2$. This cut eliminates $\sim 40\%$ of the $D^+ \rightarrow \rho^0 \mu^+ \nu$ signal, but also proves to be very effective at rejecting background consisting mostly of kaons and pions misidentified as muons.

In order to reduce systematic errors common to both modes, the $D^+ \rightarrow K^- \pi^+ \mu^+ \nu$ events used for normalization had the same vertex and muon identification cuts as in the $D^+ \rightarrow \rho^0 \mu^+ \nu$ analysis. The kaon is identified by requiring that the kaon hypothesis is favored over the pion hypothesis by at least two units of log-likelihood. The pion candidate is identified by requiring that the pion hypothesis for this track be favored over the kaon hypothesis. Background from $D^{*+} \rightarrow D^0 \pi^+ \rightarrow (K^- \mu^+ \nu) \pi^+$ is reduced by requiring $M(K^- \pi^+ \mu^+) - M(K^- \mu^+) > 0.20 \text{ GeV}/c^2$. A cut on the visible mass of $1.0 \text{ GeV}/c^2 < M(K^- \pi^+ \mu^+) < 1.8 \text{ GeV}/c^2$ suppresses background from muon misidentification.

3 BR Determination

The $D^+ \rightarrow \rho^0 \mu^+ \nu$ yield is estimated using a binned maximum log-likelihood fit of the $\pi^+ \pi^-$ invariant mass. The likelihood is defined as:

$$\mathcal{L} = \prod_{i=1}^{\# \text{bins}} \frac{n_i^{s_i} e^{-n_i}}{s_i!} \times \text{penalty} \quad (1)$$

where s_i is the number of events in bin i of the data histogram, n_i is the number of events in bin i of the fit histogram, and a penalty term, described below, is used to set a loose constraint on a known branching ratio.

The fit histogram is composed of: binned, normalized shapes of signal and background components obtained from Monte Carlo simulations, S_x , the number of events as estimated by the fit for each shape, Y_x , and the number of events that occur due to feed-down from the Cabibbo-favored decay $D^+ \rightarrow K^- \pi^+ \mu^+ \nu$. The number of events in each bin is then:

$$n_i = Y_{D^+ \rightarrow \rho^0 \mu^+ \nu} S_{\rho^0 \mu^+ \nu} + \text{ECY}_{D^+ \rightarrow K^- \pi^+ \mu^+ \nu} \epsilon(K \pi \mu \nu \rightarrow \rho \mu \nu) S_{K \pi \mu \nu} + \\ Y_{D^+ \rightarrow K_S^0 \mu^+ \nu} S_{K_S^0 \mu^+ \nu} + Y_{D^+ \rightarrow \omega \mu^+ \nu} S_{\omega \mu^+ \nu} + Y_{D_s^+} S_{D_s^+} + Y_C S_C + Y_M S_M \quad (2)$$

where the terms in Eq. 2 are explained in detail below.

As mentioned before, the shapes for the signal and background are obtained via Monte Carlo simulation. The Monte Carlo is based on Pythia 6.127 [21] and contains all known charm decays with their corresponding branching ratios and careful simulation of known secondary processes. After an event is generated, it is passed through a simulation of the FOCUS spectrometer. The events are then selected in the same way as the data.

$Y_{D^+ \rightarrow \rho^0 \mu^+ \nu}$ is the yield of the $D^+ \rightarrow \rho^0 \mu^+ \nu$ signal. $\text{ECY}_{D^+ \rightarrow K^- \pi^+ \mu^+ \nu}$ is the efficiency-corrected yield (ECY) for $D^+ \rightarrow K^- \pi^+ \mu^+ \nu$. This quantity is the estimated number of $D^+ \rightarrow K^- \pi^+ \mu^+ \nu$ events produced by FOCUS. This, along with the Monte Carlo efficiency for a $D^+ \rightarrow K^- \pi^+ \mu^+ \nu$ event to be misidentified as a $D^+ \rightarrow \rho^0 \mu^+ \nu$ event, $\epsilon(K \pi \mu \nu \rightarrow \rho \mu \nu)$, provide an estimate of the amount of feed-down of this mode into our signal. The ECY is fixed in the fit to the value obtained from the $D^+ \rightarrow K^- \pi^+ \mu^+ \nu$ analysis used for the normalization mode. $Y_{D^+ \rightarrow K_S^0 \mu^+ \nu}$ is the yield of a small $K_S^0 \rightarrow \pi^+ \pi^-$ component.

$Y_{D^+ \rightarrow \omega \mu^+ \nu}$ is the yield of $D^+ \rightarrow \omega \mu^+ \nu$, where the ω could decay either to $\pi^+ \pi^- \pi^0$ or to $\pi^+ \pi^-$. We use the recent CLEO-c collaboration measurements of the absolute branching ratio of $D^+ \rightarrow \bar{K}^{*0} e^+ \nu$ and $D^+ \rightarrow \omega e^+ \nu$ [22] to set a loose constraint on the yield of $D^+ \rightarrow \omega \mu^+ \nu$. To this end, we add a penalty

term to the likelihood of the form³

$$\exp \left[-\frac{1}{2} \left(R_{\omega/\overline{K}^{*0}} \text{ECY}_{D^+ \rightarrow \overline{K}^{*0} \mu^+ \nu} - Y_{D^+ \rightarrow \omega \mu^+ \nu} \right)^2 / \sigma_{D^+ \rightarrow \omega e \nu}^2 \right] \quad (3)$$

where $R_{\omega/\overline{K}^{*0}} = \frac{\text{BR}(D^+ \rightarrow \omega e^+ \nu)}{\text{BR}(D^+ \rightarrow \overline{K}^{*0} e^+ \nu)}$. The $\sigma_{D^+ \rightarrow \omega e \nu}$ error used in Eq. 3 is based on the errors in the branching fractions reported by CLEO-c with statistical and systematic errors added in quadrature to the error in the efficiency corrected yield for $D^+ \rightarrow \overline{K}^{*0} \mu^+ \nu$.

$Y_{D_s^+}$ is the combined yield of the modes $D_s^+ \rightarrow \eta' \mu \nu$, $D_s^+ \rightarrow \eta \mu \nu$, and $D_s^+ \rightarrow \phi \mu^+ \nu$ with η' decaying to either $\rho^0 \gamma$ or to $\eta \pi^+ \pi^-$, η decaying to either $\pi^+ \pi^- \pi^0$ or to $\pi^+ \pi^- \gamma$, and ϕ decaying to $\rho \pi$. These modes are generated simultaneously with their corresponding relative branching ratios, and a single shape, $S_{D_s^+}$, is obtained.

Y_C is the number of combinatorial background events where at least one of the three charged tracks forming the decay vertex does not belong to the vertex. After applying our selection criteria, this background is dominated by charm decays. In order to generate S_C , the combinatorial background shape, we use a large Monte Carlo sample which simulates all known charm decays, where after an event is selected the reconstructed tracks are matched against the generated tracks. If one of the reconstructed tracks does not belong to the generated decay vertex, the event is flagged as a combinatorial background event.

The last term of Eq. 2, Y_M , is the number of events due to muon misidentification. The muon misidentification shape is also obtained from a large Monte Carlo sample where all known charm decays are simulated. In this case tracks within the acceptance of the inner muon system with a confidence level less than 1% and momentum greater than 10 GeV/ c are taken as muons. This allows us to use the same selection as in the analysis, but with very few real semi-muonic decays in the sample. This shape is then weighted with a momentum-dependent misidentification probability function to obtain the final shape used in the fit. The same technique, applied to a sub-sample of the FOCUS data, gave a shape in very good agreement with the shape used in the fit. We choose not to use shape or Y_M estimates from the data due to the limited statistics available. Instead, we allow Y_M to float freely in the fit.

The $D^+ \rightarrow K^- \pi^+ \mu^+ \nu$ yield used for the normalization is estimated in the same way as the $D^+ \rightarrow \rho^0 \mu^+ \nu$ yield. In this case, we only need two components in the fit: one for the signal and one for the background. This background shape is obtained from a Monte Carlo sample where all known charm decays, except $D^+ \rightarrow K^- \pi^+ \mu^+ \nu$, are generated. The fit to the $K^- \pi^+$ line shape is similar

³ Here we have assumed that the electronic and muonic rates are equal.

to the one used in [23], and though this fit does not describe the complex line shape presented in [24], we find that it provides a robust estimate of the $D^+ \rightarrow K^- \pi^+ \mu^+ \nu$ yield.

From our fit we find 320 ± 44 $D^+ \rightarrow \rho^0 \mu^+ \nu$ events and $11,372 \pm 161$ $D^+ \rightarrow K^- \pi^+ \mu^+ \nu$ events. In Fig. 1 we show the fit result. The ratio of branching ratios is defined as

$$\frac{\text{BR}(D^+ \rightarrow \rho^0 \mu^+ \nu)}{\text{BR}(D^+ \rightarrow \bar{K}^{*0} \mu^+ \nu)} = \frac{Y_{D^+ \rightarrow \rho^0 \mu^+ \nu} / \epsilon_{D^+ \rightarrow \rho^0 \mu^+ \nu}}{Y_{D^+ \rightarrow K^- \pi^+ \mu^+ \nu} / \epsilon_{D^+ \rightarrow K^- \pi^+ \mu^+ \nu}} \times \text{BR}(\bar{K}^{*0} \rightarrow K^- \pi^+). \quad (4)$$

This branching ratio must be corrected to account for the $(5.30 \pm 0.74_{-0.96}^{+0.99})\%$ non-resonant S-wave contribution present in the $D^+ \rightarrow K^- \pi^+ \mu^+ \nu$ spectrum previously reported by FOCUS [20,24]. Including this correction, with errors added in quadrature, we find

$$\frac{\text{BR}(D^+ \rightarrow \rho^0 \mu^+ \nu)}{\text{BR}(D^+ \rightarrow \bar{K}^{*0} \mu^+ \nu)} = 0.0412 \pm 0.0057.$$

Decay Mode	Total Yield	Yield in signal region
$D^+ \rightarrow \rho^0 \mu^+ \nu$	320 ± 44	282
$D^+ \rightarrow K^- \pi^+ \mu^+ \nu$	68 ^a	44
$D^+ \rightarrow K_S^0 \mu^+ \nu$	7 ± 6	0
D_s^+ modes total	179 ± 40	101
$D^+ \rightarrow \omega \mu^+ \nu$	51 ± 22	10
Muon Mis-Id	550 ± 44	263
Combinatoric	233 ± 50	99

^a The $D^+ \rightarrow K^- \pi^+ \mu^+ \nu$ yield is not a fit parameter, instead it is estimated based on the efficiency for a $D^+ \rightarrow K^- \pi^+ \mu^+ \nu$ event to be reconstructed as a $D^+ \rightarrow \rho^0 \mu^+ \nu$ event as described in the text.

Table 1

Contributions to the $\pi^+ \pi^-$ invariant mass spectrum. The third column shows the number of events in the signal region defined as $0.62 \text{ GeV}/c^2 < M(\pi^+ \pi^-) < 0.92 \text{ GeV}/c^2$.

Many tests were performed to ensure that the final result is stable to our detailed cut choice, as well as a good representation of the data. The quantitative tests we performed to determine additional sources of uncertainty are detailed below.

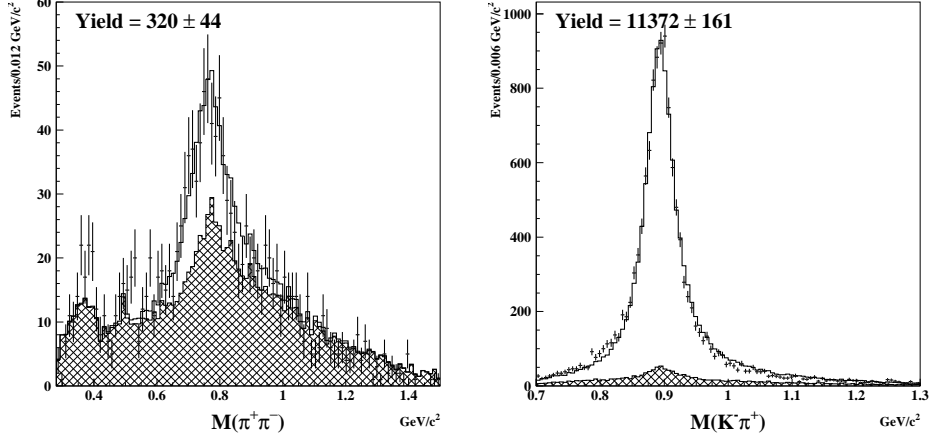


Fig. 1. Fit to the $\pi^+\pi^-$ invariant mass (left) and the $K^-\pi^+$ invariant mass (right). The fit to the data (error bars) is shown as a solid line. The hatched histogram on invariant mass plots is the background.

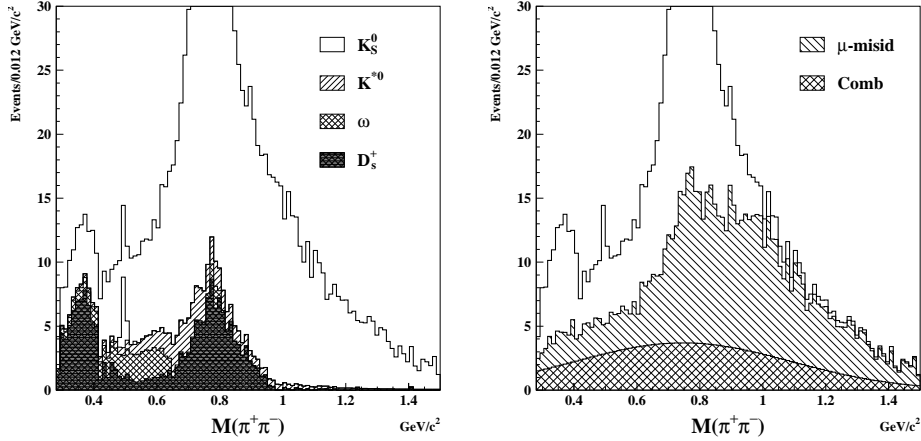


Fig. 2. $M(\pi^+\pi^-)$ background contributions shown in cumulative plots. Left: semileptonic contributions. Right: Muon misid and combinatorial background contributions. In the case of the $D^+ \rightarrow \bar{K}^{*0} \mu^+ \nu$ and combinatorial backgrounds, smoothed shapes been used. The fit histogram is shown in both plots for reference.

4 Systematic Studies

Several studies have been performed in order to assess systematic contributions to the uncertainty in the ratio. Three possible contributions have been identified.

The first contribution is due to the final cut selection used to determine the branching ratio. In order to estimate a contribution from this source, we vary our cuts around the final choice to exercise likely differences between the signal and background. Since the D^+ is long lived compared to sources of background from D_s^+ , and other short-lived backgrounds such as those coming

from non-charm sources, we vary the significance of the separation between the production and the decay vertices from 10σ to 20σ , and out of target requirements for the decay vertex from 0σ to 2σ . To look for poorly formed vertices and vertices that are formed from particles that decay into muons early in the spectrometer, we vary the confidence level of the secondary vertex from 1% to 10%. We have estimated the feed-down from $D^+ \rightarrow K^- \pi^+ \mu^+ \nu$ using our Monte Carlo simulation, but look for backgrounds we might have missed by varying the Čerenkov identification cuts for the pions from 4 to 6 units of likelihood. The level of the muon misid was checked by changing the muon identification confidence level from 1% to 10%, the muon momentum cut from 10 GeV/ c to 20 GeV/ c , and selecting events that left hits in all 6 of the muon planes. A very stringent test which dramatically changes the background level is to relax the visible mass cut. Though the statistical significance of the result suffers due to the inclusion of so much background, this is an important check on backgrounds we might have missed coming from higher multiplicity modes, which are expected to be small, and combinatorial sources.

The cut systematic is assessed by measuring the branching ratio for the different cut combinations and calculating the sample variance for the returned values of $\frac{\text{BR}(D^+ \rightarrow \rho^0 \mu^+ \nu)}{\text{BR}(D^+ \rightarrow \overline{K}^{*0} \mu^+ \nu)}$. Because our tested cuts have succeeded in delivering a broad range of signal to background values as well as changes in the final yield, this method is likely to deliver a conservative estimate of the systematic error due to our cut selection. We find no significant change in the branching ratio due to our particular cut choice and assign a systematic uncertainty of 0.0023 due to our cut selection.

The second contribution is related to our fit. In order to check the fit against possible biases as well as the accuracy of the statistical error reported by the fit, we perform the fit multiple times after fluctuating each bin of the data histogram using a Poisson distribution. We find that both the mean and width of the distribution of the fit results are in agreement with our reported results.

We test the effect of the fit inputs by changing the $D^+ \rightarrow K^- \pi^+ \mu^+ \nu$ ECY used to estimate the amount of background due to K/π misidentification in our $D^+ \rightarrow \rho^0 \mu^+ \nu$ sample by a factor of two and by fitting with no restrictions on the $D^+ \rightarrow \omega \mu^+ \nu$ yield. We test the combined D_s^+ shape used in the fit by fitting our signal using the individual shapes of the D_s^+ modes mentioned earlier. In this case, we replace the D_s^+ yield parameter in the fit with a parameter representing the $D_s^+ \rightarrow \phi \mu^+ \nu$ ECY and we extract the individual yields using the branching ratios of these modes relative to $D_s^+ \rightarrow \phi \mu^+ \nu$. These branching ratios are then varied by $\pm 1\sigma$. We have also changed the shape of the combinatorial background by replacing it with the shape obtained when two same sign pions are used to form a $\pi\pi\mu$ vertex. As a final check on the fit, we have changed the binning scheme and mass range used in the fit. As in the case of cut variations, we calculate the sample variance of the returned values and quote this as our systematic contribution. We find this contribution to be

0.0038 mostly coming from the uncertainty in the combinatorial background shape.

The third category includes a search for additional, unaccounted for, systematic uncertainty that may come from the detector simulation and/or the charm production mechanism. We estimate this by splitting our sample into three pairs of statistically independent sub-samples. A powerful test for the production model, trigger, and detector simulation for the signal as well as for the background is to split the data according to the D^\pm momentum. Another test of the production model is to look whether we have a decay of a D^+ or a D^- . Our final split sample looks at two different detector configurations. For roughly 30% of the FOCUS running we ran without the interleaved silicon planes within the target. With this split, we tested the detector simulation as well as lifetime dependent backgrounds.

In order to separate the likely systematic error contribution in any differences in the results from larger statistical fluctuations due to reduced statistics, FOCUS uses a technique based on the *S-factor* method of the PDG. In this method the branching ratio is measured for each pair of split sub-samples and a scaled variance is calculated. The split sample contribution is the difference between the scaled variance and the statistical variance if the scaled variance is greater than the statistical variance for the entire sample. We find that no additional contribution to the systematic uncertainty is indicated by this search.

The total systematic uncertainty is obtained by adding in quadrature all of these contributions as summarized in Table 2.

Systematic Source	Error
Cut variations	0.0023
Fit variation	0.0038
Total	0.0044

Table 2

Sources of systematic errors. The three sources are added in quadrature to obtain the total systematic error.

5 Conclusions

From $320 \pm 44 D^+ \rightarrow \rho^0 \mu^+ \nu$ decays and $11,372 \pm 161 D^+ \rightarrow K^- \pi^+ \mu^+ \nu$ decays, we report a measurement of the branching ratio

$$\frac{\text{BR}(D^+ \rightarrow \rho^0 \mu^+ \nu)}{\text{BR}(D^+ \rightarrow \overline{K}^{*0} \mu^+ \nu)} = 0.041 \pm 0.006 \text{ (stat.)} \pm 0.004 \text{ (syst.)}.$$

Using this result along with the FOCUS measurement of the ratio $\frac{\text{BR}(D^+ \rightarrow \overline{K}^{*0} \mu^+ \nu)}{\text{BR}(D^+ \rightarrow K^- \pi^+ \pi^+)}$ [25], the PDG [16] value of the absolute branching fraction of the decay $D^+ \rightarrow K^- \pi^+ \pi^+$, and the FOCUS measurement of the D^+ lifetime [26], we calculate

$$\Gamma(D^+ \rightarrow \rho^0 \mu^+ \nu) = (0.22 \pm 0.03 \pm 0.02 \pm 0.01) \times 10^{10} \text{ s}^{-1}$$

where the last error is a combination of the uncertainties on the quantities not measured in this work. When calculating the partial decay width, we have corrected $\frac{\text{BR}(D^+ \rightarrow \overline{K}^{*0} \mu^+ \nu)}{\text{BR}(D^+ \rightarrow K^- \pi^+ \pi^+)}$ with the updated value for the S-wave non-resonant contribution [24]. In Table 3 and Table 4, we compare our result to previous experimental results and theoretical predictions, respectively.

Our result for $\frac{\text{BR}(D^+ \rightarrow \rho^0 \mu^+ \nu)}{\text{BR}(D^+ \rightarrow \overline{K}^{*0} \mu^+ \nu)}$ is consistent with a recent CLEO collaboration result on the absolute branching ratios for D^+ semi-electronic decays [22] and represents a significant improvement to the world average for the semi-muonic mode. The experimental results indicate that the QCD Sum Rule predictions for $D^+ \rightarrow \rho^0 \ell^+ \nu$ [1,5] are too low.

Reference	$\frac{\text{BR}(D^+ \rightarrow \rho^0 \mu^+ \nu)}{\text{BR}(D^+ \rightarrow \overline{K}^{*0} \mu^+ \nu)}$	$\frac{\text{BR}(D^+ \rightarrow \rho^0 e^+ \nu)}{\text{BR}(D^+ \rightarrow \overline{K}^{*0} e^+ \nu)}$
E653 [13]	$0.044_{-0.029}^{+0.034}$	
E687 [14]	0.079 ± 0.023	
E791 [15]	0.051 ± 0.017	0.045 ± 0.017
CLEO [22]		0.038 ± 0.008
This result	0.041 ± 0.007	

Table 3

Experimental results for the branching ratio. Statistical and systematic errors have been added in quadrature.

6 Acknowledgments

We wish to acknowledge the assistance of the staffs of Fermi National Accelerator Laboratory, the INFN of Italy, and the physics departments of the collaborating institutions. This research was supported in part by the U. S. National Science Foundation, the U. S. Department of Energy, the Italian Istituto Nazionale di Fisica Nucleare and Ministero dell'Università e della Ricerca Scientifica e Tecnologica, the Brazilian Conselho Nacional de Desenvolvimento Científico e Tecnológico, CONACyT-México, the Korean Ministry of Education, and the Korea Research Foundation.

Reference	ℓ	$\frac{\text{BR}(D^+ \rightarrow \rho^0 \ell^+ \nu)}{\text{BR}(D^+ \rightarrow \overline{K}^{*0} \ell^+ \nu)}$	$\Gamma(D^+ \rightarrow \rho^0 \ell^+ \nu) (10^{10} \text{ s}^{-1})$
Ball [1] (SR)	e		0.06 ± 0.02
APE [2] (LQCD)	ℓ	0.043 ± 0.018	0.3 ± 0.1
Jaus [3] (QM)	ℓ	0.030	0.16
ISGW2 [4] (QM)	e	0.023	0.12
Yang–Hwang [5] (SR)	e	0.018 ± 0.005	$0.07^{+0.04}_{-0.02}$
O’Donnell–Turan [6] (LF)	μ	0.025	
Melikhov [7] (QM)	ℓ	0.027, 0.024	0.15, 0.13
Ligeti–Stewart–Wise [8]	ℓ	0.044	
Kondratyuk–Tchein [9] (LF)	ℓ	0.035, 0.033, 0.033, 0.032	0.19, 0.20, 0.18, 0.19
Melikhov–Stech [10] (QM)	ℓ	0.035	0.21
Wang–Wu–Zhong [11] (LC)	ℓ	0.035 ± 0.011	0.17 ± 0.04
Fajfer–Kamenik [12]	ℓ	0.045	0.25
This result	μ	0.041 ± 0.007	0.22 ± 0.04

Table 4

Theoretical predictions for the branching ratio and partial decay width. Most of the theoretical predictions are calculated for $D^0 \rightarrow \rho^- \ell^+ \nu$. To compare these predictions with our result, we have used the isospin conjugate relation $\Gamma(D^+ \rightarrow \rho^0 \ell^+ \nu) = 1/2 \Gamma(D^0 \rightarrow \rho^- \ell^+ \nu)$.

References

- [1] P. Ball, Semileptonic Decays $D \rightarrow \pi(\rho)e\nu$ and $B \rightarrow \pi(\rho)e\nu$ from QCD Sum Rules, Phys. Rev. D 48 (1993) 3190.
- [2] C. R. Allton et al., Lattice Calculation of D and B Meson Semileptonic Decays, Using the Clover Action at $\beta = 6.0$ on APE, Phys. Lett. B 345 (1995) 513.
- [3] W. Jaus, Semileptonic, Radiative and Pionic decays of B, B* and D, D* Mesons, Phys. Rev. D 53 (1996) 1349.
- [4] N. Igsur and D. Scora, Semileptonic Meson Decays in the Quark Model: An Update, Phys. Rev. D 52 (1995) 2783.
- [5] W. Y. Wang, Y. L. Wu and M. Zhong, The QCD Sum Rule Approach for the Semileptonic Decay of the D or B Meson into a light meson and leptons, Z. Phys, C 73 (1997) 275.
- [6] P. J. O’Donnell and G. Turan, Charm and Bottom Semileptonic Decays, Phys. Rev. D 56 (1997) 295.
- [7] D. Melikhov, Exclusive Semileptonic Decays of Heavy Mesons in the Quark Model, Phys. Lett. B 394 (1997) 385.

- [8] Z. Ligeti, I. W. Stewart and M. B. Wise, Comment on V_{ub} from Exclusive Semileptonic B and D Decays, Phys. Lett. B 420 (1998) 359.
- [9] L. A. Kondratyuk and D. V. Tchekin, Transition Form Factors and Probabilities of the Semileptonic Decays of B and D Mesons within Covariant Light-Front Dynamics, Phys. Atom. Nucl. 64 (2001) 727.
- [10] D. Melikhov and B. Stech, Weak Form Factors for Heavy Meson Decays: An Update, Phys. Rev. D 62 (2000) 014006.
- [11] W. Y. Wang, Y. L. Wu and M. Zhong, Heavy to Light Meson Exclusive Semileptonic Decays in Effective Field Theory of Heavy Quarks, Phys. Rev. D 67 (2003) 014024.
- [12] S. Fajfer and J. Kamenik, Charm Meson Resonances and $D \rightarrow V$ Semileptonic Form Factors, Phys. Rev. D 72 (2005) 034029.
- [13] K. Kodama et al., Observation of $D^+ \rightarrow \rho(770)^0 \mu^+ \nu$, Phys. Lett. B 316 (1993) 455.
- [14] P. L. Frabetti et al., Observation of the Vector Meson Cabibbo Suppressed Decay $D^+ \rightarrow \rho^0 \mu^+ \nu$, Phys. Lett. B 391 (1997) 235.
- [15] E. M. Aitala et al., Measurement of the Branching Ratio $\frac{B(D^+ \rightarrow \rho^0 l^+ \nu_l)}{B(D^+ \rightarrow K^{*0} l^+ \nu_l)}$, Phys. Lett. B 397 (1997) 325.
- [16] S. Eidelman et al., Review of Particle Physics, Phys Lett. B 592 (2004) 1.
- [17] P. L. Frabetti et al., Description and Performance of the Fermilab E687 Spectrometer, Nucl. Instrum. Meth. A 320 (1992) 519.
- [18] J. M. Link et al., The Target Silicon Detector for the FOCUS Spectrometer, Nucl. Instrum. Meth. A 516 (2004) 364.
- [19] J. M. Link et al., Čerenkov Identification in FOCUS, Nucl. Instrum. Meth. A 484 (2002) 270.
- [20] J. M. Link et al., Evidence for New Interference Phenomena in the Decay $D^+ \rightarrow K^- \pi^+ \mu^+ \nu$, Phys. Lett. B 535 (2002) 43.
- [21] T. Sjöstrand, High Energy Physics Event Generation with PYTHIA 5.7 and JETSET 7.4, Comp. Phys. Comm 82 (1994) 74.
- [22] G. S. Huang et al., Absolute Branching Fraction Measurements of Exclusive D^+ Semileptonic Decays, hep-ex/0506053 .
- [23] J. M. Link et al., Measurement of the Ratio of the Vector to Pseudoscalar Charm Semileptonic Decay Rate $\frac{\Gamma(D^+ \rightarrow \overline{K}^{*0} \mu^+ \nu)}{\Gamma(D^+ \rightarrow \overline{K}^0 \mu^+ \nu)}$, Phys. Lett. B 598 (2004) 33.
- [24] J. M. Link et al., Hadronic Mass Spectrum Analysis of $D^+ \rightarrow K^- \pi^+ \mu^+ \nu$ Decay and Measurement of the $K^*(892)^0$ Mass and Width, Phys. Lett. B 320 (2005) 72.

- [25] J. M. Link et al., New Measurement of the $\frac{\Gamma(D^+ \rightarrow \overline{K}^{*0} \mu^+ \nu)}{\Gamma(D^+ \rightarrow K^- \pi^+ \pi^+)}$ and $\frac{\Gamma(D_S^+ \rightarrow \phi \mu^+ \nu)}{\Gamma(D_S^+ \rightarrow \phi \pi^+)}$, Phys. Lett. B 541 (2002) 243.
- [26] J. M. Link et al., New Measurement of the D^0 and D^+ lifetimes, Phys. Lett. B 537 (2002) 192.